

## NUMERICAL AND EXPERIMENTAL STUDY OF THE ROCKING RESPONSE OF UNANCHORED BODY TO HORIZONTAL BASE EXCITATION

G.C. Manos<sup>1\*</sup>, A. Petalas<sup>1</sup>, M. Demosthenous<sup>1</sup>

<sup>1</sup>Laboratory of Strength of Materials and Structures  
Dept. Civil Engineering, Aristotle University of Thessaloniki  
University Campus, Egnatia street, Thessaloniki, 54006  
gcmanos@civil.auth.gr

**Keywords:** Rocking, Rigid Body, Numerical Simulation Experimental Verification, Ancient Monuments

**Abstract.** *Ancient Greek and Roman structures composed of large heavy members that simply lie on top of each other in a perfect-fit construction without the use of connecting mortar, are distinctly different from relatively flexible contemporary structures. The colonnade (including free standing monolithic columns or columns with drums) is the typical structural form of ancient Greek or Roman temples. The seismic response mechanisms that develop on this solid block structural system during strong ground motions can include sliding and rocking, thus dissipating the seismic energy in a different way from that of conventional contemporary buildings. This paper presents results and conclusions from an experimental study that examines the dynamic response of rigid bodies, representing simple models of ancient columns. These models are subjected to various types of horizontal base motions (including sinusoidal as well as earthquake base motions), reproduced by the Earthquake Simulator Facility of Aristotle University. The employed rigid bodies were made of steel and are assumed to be models of prototype structures 20 times larger. In addition to the experimental study, numerical simulations of the observed dynamic and earthquake rocking response of the free standing steel rigid block specimens were also carried out. These numerical simulations were performed in two different ways. At first, a specific software was developed based on analytical expressions of the equations of motion for this problem together with numerical integration techniques that yielded predictions of the rocking response. Next, the numerical simulation employed a commercial finite element software package (Abaqus) and utilized the capabilities of this software to obtain predictions of the rocking response of the tested in the laboratory free standing steel rigid block specimens. The numerical results obtained from these two different numerical simulations are presented and compared with the experimental response measurements as well as among each other. From this comparison the reliability of these two distinct numerical simulations is presented and discussed.*

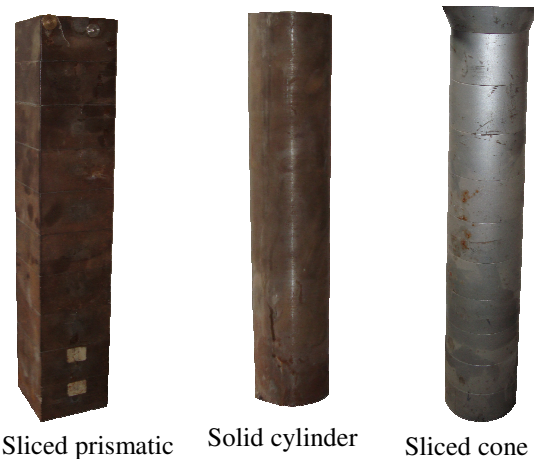
## 1 INTRODUCTION

Ancient Greek and Roman structures composed of large heavy members that simply lie on top of each other in a perfect-fit construction without the use of connecting mortar, are distinctly different from relatively flexible contemporary structures. The colonnade (including free standing monolithic columns or columns with drums) is the typical structural form of ancient Greek or Roman temples ([7], [8], [9]). The columns are connected at the top with the epistyle (entablature), also composed of monolithic orthogonal blocks, spanning the distance between two columns (figure 1a).

The seismic response mechanisms that develop on this solid block structural system during strong ground motions can include sliding and rocking, thus dissipating the seismic energy in a different way from that of conventional contemporary buildings ([4], [6]). This paper presents results and conclusions from an extensive experimental study that examines the dynamic response of rigid bodies, representing simple models of ancient columns or colonnades. These models are subjected to various types of horizontal base motions (including sinusoidal as well as earthquake base motions), reproduced by the Earthquake Simulator Facility of Aristotle University. The rigid bodies employed in this study were made of steel and are assumed to be models of prototype structures 20 times larger ([6]). The basic configuration that is examined here is that of a single steel prismatic model. Apart from this model, additional models of cylindrical as well as of a truncate cone form were also studied (see figure 1b) but not reported here. Dynamic and simulated earthquake rocking response results are presented in a summary form, mainly in section 2, obtained from an extensive investigation employing these monolithic free-standing rigid models [6]. The measured response is next compared with predictions from numerical simulations that employed software developed at Aristotle University (termed analytical results, [4], [6], section 3). Finally, numerical predictions of the dynamic and simulated earthquake rocking response of the prismatic model, as obtained by applying the commercial software abaqus are also presented and compared with the experimental and analytical results.

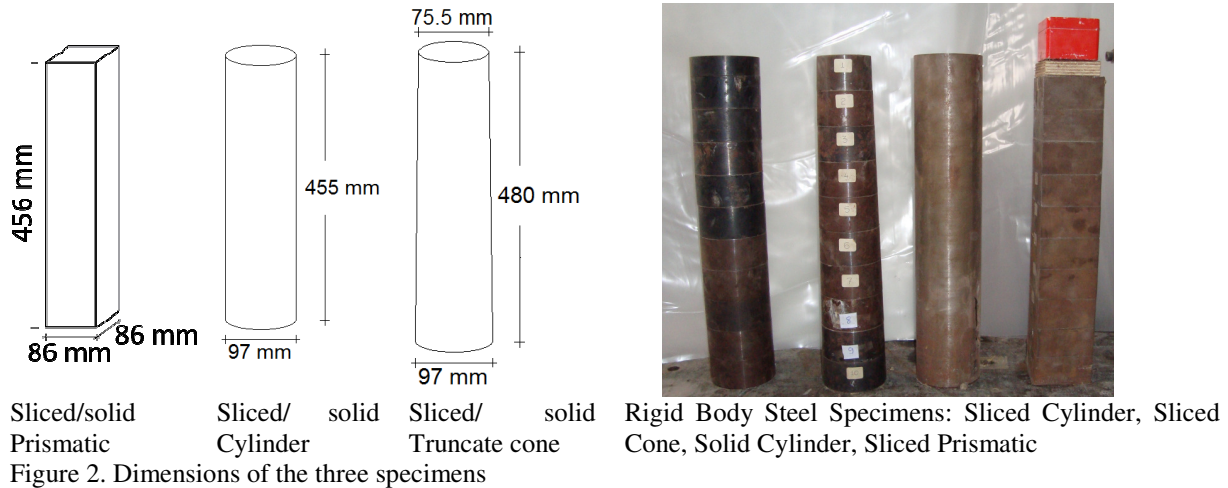


Figure 1a. The Temple of Zeus, Ancient Corinth



Sliced prismatic      Solid cylinder      Sliced cone

Figure 1a. The characteristics of the three specimens



Specimen	Mass (kg)	Side length / diameter (mm)	Height (mm)	Distance center of mass from rocking pole (mm)	Critical Rocking Angle (rad)	Mass Moment of Inertia-rocking pole $\text{kg m}^2$	Natural Rocking Frequency (rad/sec)
Prismatic	26.10	86	456	232	0.1886	1.873	5.631
Cylindrical	26.30	97	455	227	0.2132	1.883	5.631
Truncate cone	21.94	75.5 / 97	480	220	0.2203	1.527	5.631

Table 1. Basic parameters for the rocking response of the three specimens.

## 2 INVESTIGATION OF THE DYNAMIC RESPONSE OF A SOLID RIGID BODY

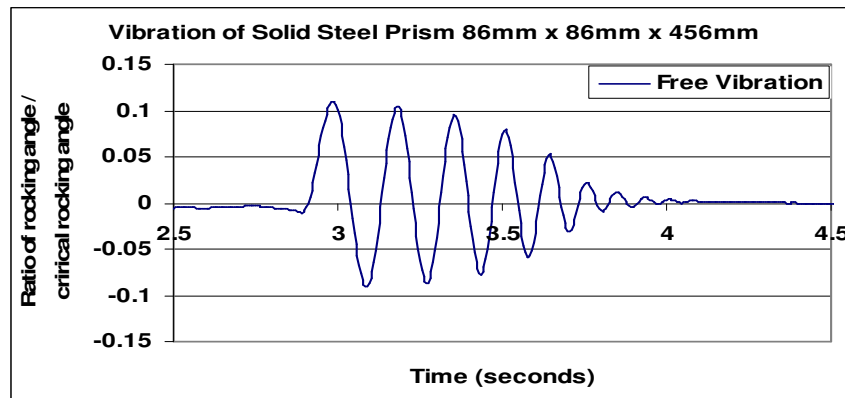
The dimensions of the examined rigid models, are shown in figure 2. These specimens were placed on the earthquake simulator simply free-standing on the horizontal moving platform of the shaking table. A very stiff, light metal frame was built around each studied model in order to carry the displacement transducers that measured the rocking angle; this metal frame also provided temporary support to the specimen during excessive rocking displacements indicating overturning.

The dynamic behaviour of each specimen was governed by its rocking response. The experimental investigation of its rocking response included periodic sine-wave tests with a chosen range of frequencies and amplitudes as well as earthquake simulated tests using the El Centro 1940 record. A simple way to estimate the dissipation of energy during rocking is to obtain the value of the coefficient of restitution by comparing free vibration rocking response measurements with those predicted numerically. From such comparisons the coefficient of restitution was obtained with the value that yields the best agreement between measured response parameters and results from a numerical solution outlined in section 3.

The numerical solutions employed were verified for their stability and convergence through an extensive parametric study that examined various methods of numerical integration and time step. This correlation was next extended with measurements from sinusoidal as well as earthquake simulated tests (section 3). The numerical studies in this case employed the same base excitations recorded at the Earthquake Simulator during the tests and used as values for the coefficient of restitution the ones determined from the same experimental sequence and the best numerical solution that was found from the above mentioned study ([4], [5], [6]).

## 2.1. Free Vibration Tests.

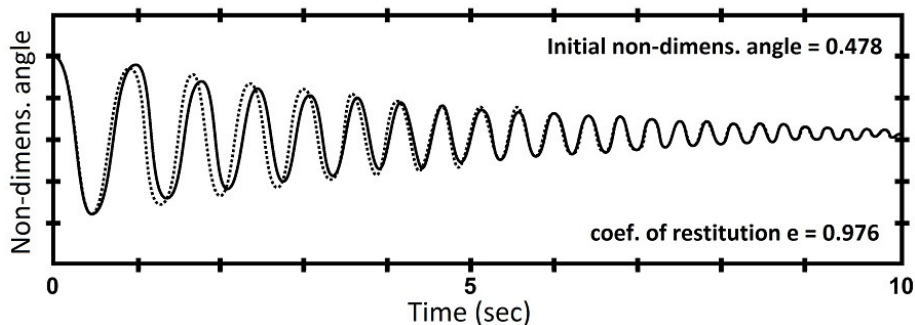
The sequence of tests for the solid truncate cone included free vibrations tests, with the objective of assessing the coefficient of restitution of the test structure. The following figure (figure 3) depicts the rocking angle response (solid line) from such a free vibration test. Superimposed on this graph with a dash line is the numerically predicted rocking response, with a coefficient of restitution value that gave the best fit to the experimental measurements. The predicted rocking response was derived from the linearised equations of the rocking motion ([1], [6]). Certain discrepancies are apparent at the initial large amplitude rocking stages. This must be attributed to three-dimensional (3-D) rocking ([3]), since rocking in a perfect plane for a 3-D model requires exacting initial conditions and the slightest out-of-plane disturbance will cause rocking to be 3-D. When the specimen tested is prismatic instead of truncate cone the 3-D response during rocking is minimized and good correlation can be obtained between observed and predicted behaviour thus assessing more accurately the coefficient of restitution ([4], [6]). A summary of the “analytical solution” is given in section 3.



a. Measure rocking response of Solid Steel Prism

Prismatic specimen

— Measured response  
 ..... Analytical solution



b. Measured and predicted free vibration rocking response of Solid Steel Prism

Figure 3. Free vibration response of the prismatic specimen and comparison with analytical predictions

## 2.2. Sinusoidal Tests

During these tests the frequency of motion was varied from 1Hz to 7Hz in steps of 1Hz from test to test. This resulted in groups of tests with constant frequency for the horizontal sinusoidal motion for each test. In the various tests belonging to the same group of constant frequency, the amplitude of the excitation was varied progressively from test to test. Figures 4a, 4b and 4c depict the rocking response of the solid specimen during this sequence of tests

for three different excitation cases for the same non-dimensional frequency  $\Omega$  having a value equal to 3.35 (see equation 1).

$$A = \frac{x}{\theta_{cr} \cdot g}, \quad \Omega = \frac{\omega}{p}, \quad p = \sqrt{\frac{W \cdot R_c}{I_o}} \quad (1)$$

- $A$  = Non-dimensional base acceleration amplitude  
 $x$  = Actual horizontal peak base acceleration of the sinusoidal motion  
 $\theta_{cr}$  = Critical angle (rad) indicating overturning of the specimen  
 $g$  = The gravitational acceleration  
 $\Omega$  = Non-dimensional frequency  
 $\omega$  = Actual sinusoidal frequency (rad/sec)  
 $p$  = The natural rocking frequency of the specimen (rad/sec)  
 $W$  = The weight of the block  
 $R_c$  = The distance of the center of gravity from the rocking pole  
 $I_o$  = The mass moment of inertia with respect to the rocking pole

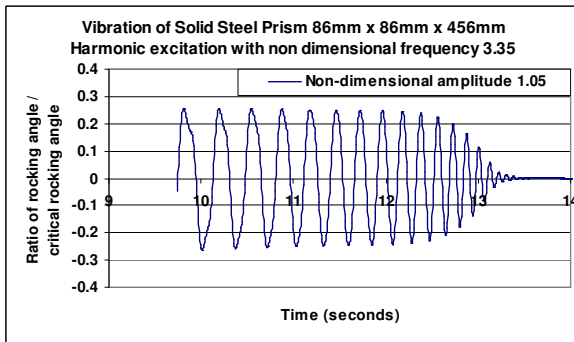


Figure 4b. Rocking response of prismatic specimen for  $\Omega=3.35$ ,  $A=1.05$

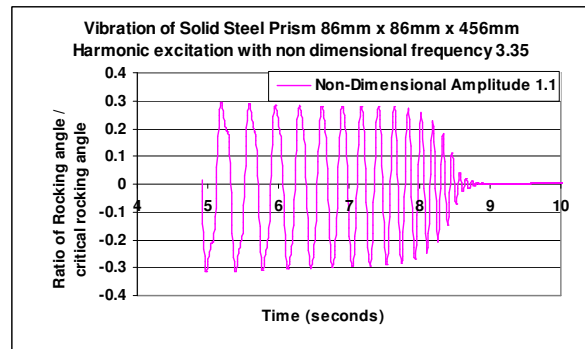


Figure 4b. Rocking response of prismatic specimen for  $\Omega=3.35$ ,  $A=1.1$

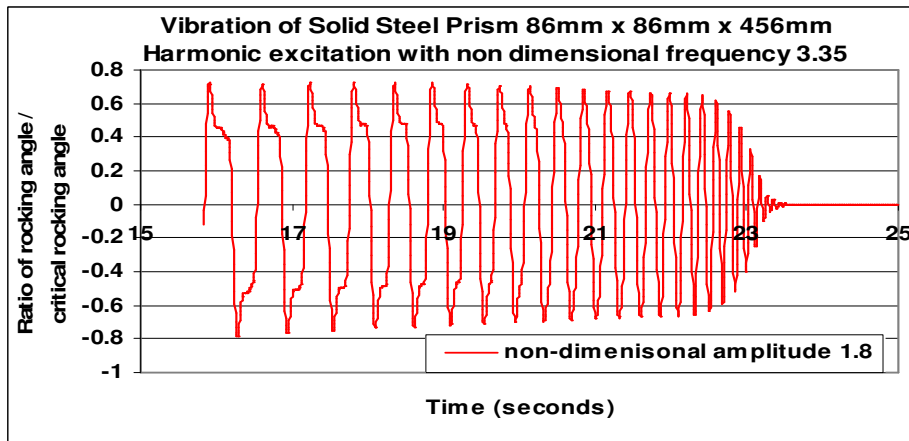


Figure 4c. Rocking response of prismatic specimen for  $\Omega=3.35$ ,  $A=1.80$

The response parameter that is plotted in figures 4a to 4c is the ratio of the rocking angle over the critical angle. For the case of the prismatic specimen the critical angle is equal to 0.1886rad. Moreover, the intensity of the excitation, as expressed by the value of the non-

dimensional amplitude  $A$ , keeps increasing from the value of 1.05 to the value of 3.35.

The following points can be made from the observed behaviour during these tests:

- For small amplitude tests the rocking behaviour is not present; the motion of the specimen in this case follows that of the base.
- As the horizontal base motion is increased in amplitude, rocking is initiated. This rocking appears to be sub-harmonic in the initial stages and becomes harmonic at the later stages.
- Further increase in the amplitude of the base motion results in excessive rocking response, which after certain buildup leads to the overturning of the specimen. At this stage, the rocking response is also accompanied by some significant sliding at the base as well as by rotation and rocking response out-of-plane of the excitation axis.

The above observations have been noted when the sinusoidal excitations were performed keeping the non-dimensional frequency value constant and equal to  $\Omega_1$  varying at the same time the non-dimensional amplitude  $A_j$  of the excitation. Each observation is termed in three distinct ways; that is: a) no-rocking, b) stable rocking, and c) unstable rocking which leads to overturning of the rigid specimen. Moreover, each of these observations corresponds to a set of non-dimensional frequency value  $\Omega_i$  and non-dimensional amplitude  $A_j$  of the excitation. If the above experiments are repeated with a new constant value of the non-dimensional frequency equal to  $\Omega_i$  varying again only the non-dimensional amplitude  $A_k$  of the excitation a new set of observations ( $\Omega_i, A_k$ ) will be obtained. For the new set of observations the comments made before will again be valid. All these sets of observations ( $\Omega_i, A_k$ ) can be depicted on a plot having as abscissa the non-dimensional frequency value  $\Omega_i$  and as ordinates the non dimensional amplitude of the base motion  $A_k$ .

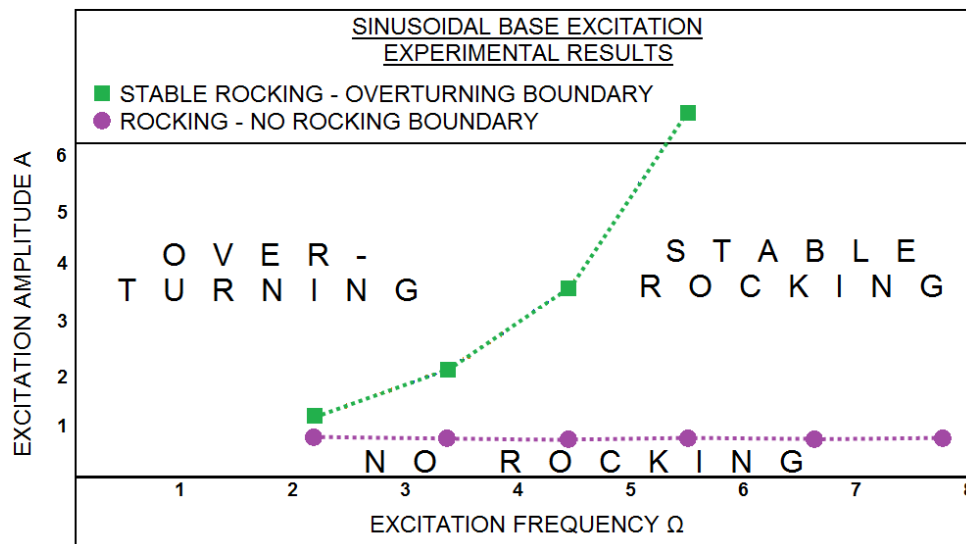


Figure 5. Mapping the stable-unstable rocking response

The above stages are graphically portrayed in the plot of figure 5 (together with the numerical results as is explained below). In this figure, the two boundaries, as established from consecutive experiments of sinusoidal vibrations of constant non-dimensional frequency  $\Omega_i$  and amplitude  $A_k$  of increasing intensity are marked. The first is the rocking-no rocking boundary, which is marked with circles; it indicates the limit state of sinusoidal vibrations that changes from no-rocking to stable rocking when the non-dimensional amplitude takes a



value that places this motion above this boundary. The second is the stable rocking-unstable rocking boundary, which is marked with squares; it indicates the limit state of sinusoidal vibrations that changes from stable rocking to overturning when the non-dimensional amplitude takes a value that places this motion above this boundary. These two boundaries have been obtained from a large number of experiments whereby the prismatic specimen has been subjected to sinusoidal base motions each time with the different value of non-dimensional frequency  $\Omega_i$  and non-dimensional amplitude  $A_k$ . The following observations summarize the main points of these two boundary lines of figure 5:

- The non-dimensional stable-unstable limit rocking amplitude values  $A_k$  increases rapidly with the non-dimensional frequency.
- For small values of the non-dimensional frequency  $\Omega_i$  the transition stage from no-rocking to overturning, in terms of non-dimensional amplitude value  $A_k$ , is very small and it occurs with minor amplitude increase.
- The no-rocking stable rocking non-dimensional amplitude values  $A_k$  remain almost constant and equal approximately to one (1) for all non-dimensional frequency values  $\Omega_i$ .

### 3 NUMERICAL SIMULATION BASED ON AN ANALYTICAL SOLUTION OF ROCKING

Initially, the numerical simulation was based on a software that was developed at the Laboratory of Strength of Materials and Structures ([4], [6]). This software was based on the integration in the time domain of the equations of motion for the rocking response of a rigid body. This solution investigated two alternative time step integration schemes that will be described in a summary in the following.

First, the simple time step integration scheme was employed whereby the equation of motion was expressed for a time step ( $t_i$ ) through the values of the unknown parameters at the previous step ( $t_{i-1}$ ). Thus, for finding the value of a function  $\Theta_i(t)$  the values of this function and its derivatives must be known at the previous time step  $\Theta(t_{i-1})$  and  $\Theta'(t_{i-1})$  (see figure 6a).

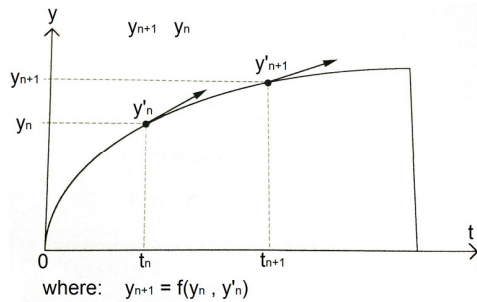


Figure 6a. Simple time step integration scheme

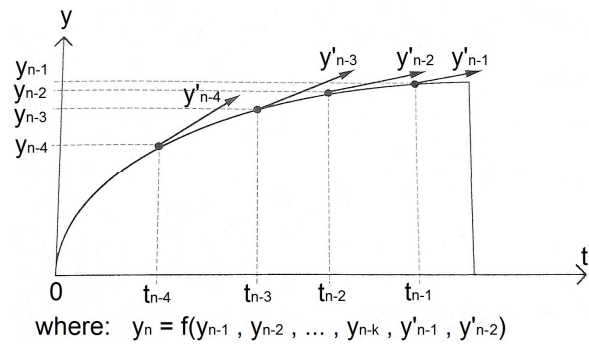


Figure 6b. Multiple time step integration scheme

Alternatively, a multiple time step integration scheme was employed, whereby for finding the value of a function  $\Theta_i(t)$  the values of this function and its derivatives must be known at a number of previous time steps  $\Theta(t_{i-1})$  and  $\Theta'(t_{i-1})$ ,  $\Theta(t_{i-2})$  and  $\Theta'(t_{i-2})$ ,  $\Theta(t_{i-3})$  and  $\Theta'(t_{i-3})$ , etc. (see figure 6b). In the framework of this investigation, the Hamming approximation was utilized whereby the value at a time step  $\Theta_i(t)$  was based on the values of four previous time steps. The first four values for every rocking cycle are obtained applying the method Runge Kutta according to Runge.

### 3.1. Sinusoidal Tests

A numerical study has been performed, aimed to simulate the dynamic response of the solid prismatic specimen, using the non-dimensional linear equations for sinusoidal excitation as given by Spanos and Koh ([2]) and with a value for the coefficient of restitution as obtained from the free vibration tests presented before. The numerical analyses have been performed for various combinations of amplitude  $A_k$  and frequency  $\Omega_i$  as was done for the experiments previously described. Figure 7 presents these results in a summary form using the same way to portray the response as was done to describe the rocking response in figure 5, observed during the experimental sequence with the horizontal sinusoidal base motion. These boundaries, that is the no-rocking stable rocking boundary and the stable-rocking-overturning boundary, are also plotted in figure 7, as predicted from the results of this numerical analysis, based on the integration of the analytical equations of rocking motion. As can be seen in figure 7, the stable rocking-overturning boundary is depicted with two boundary lines; one corresponds to smaller amplitude values  $A_k$  (lower limit, plotted with a solid line) and a second that corresponds to larger amplitude values  $A_k$  (upper limit, plotted with a dashed line). This signifies that the results of this type of numerical analysis do not define a single stable rocking - overturning boundary line as was defined by the experimental sequence.

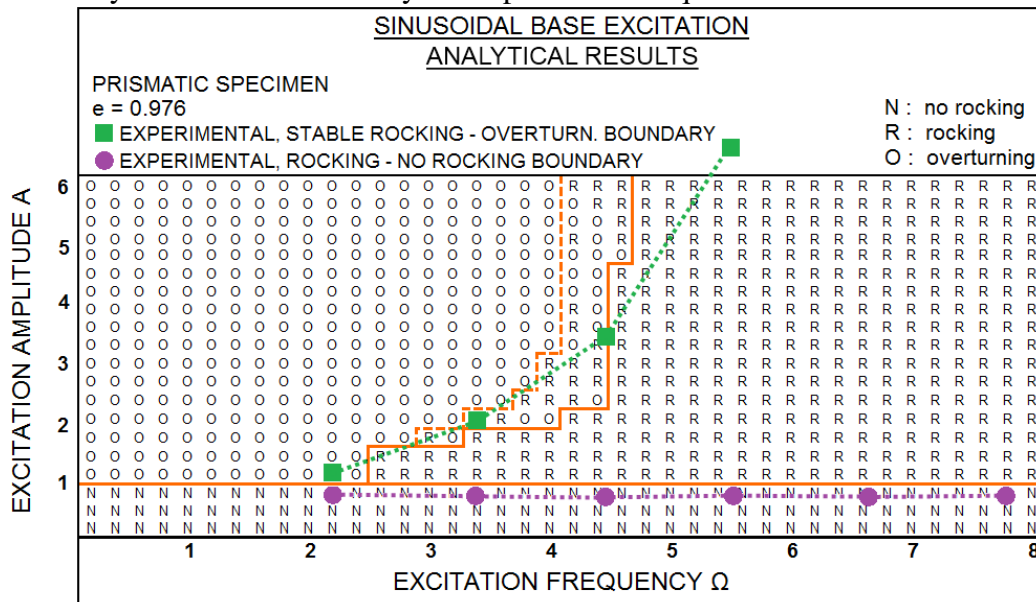


Figure 7. Mapping the stable-unstable rocking response. Analytical predictions and experimental measurements

The experimentally defined boundaries are superimposed on the analytical results in the plot of figure 7. Fairly good agreement can be seen between numerical predictions and the corresponding experimental measurements in terms of defining the two boundaries.

### 3.2. Simulated Earthquake tests

A number of tests were performed during this sequence with progressively increasing intensity, based on the 1940 El Centro Earthquake record. The intensity is measured with the indicator Span (figures 8a to 8c); higher intensity of the simulated earthquake motion corresponds to a larger value for the indicator Span. The base acceleration and displacement response was measured together with the rocking response of the tested specimen. The principal objective of these tests was to observe again the stable-unstable behaviour of the model. The



base excitations recorded at the Earthquake Simulator were used in the numerical simulation of the earthquake response; the value for the coefficient of restitution was taken from the free vibration tests. The full time history of the predicted rocking angle response is compared with the corresponding measured rocking angle in figures 8a to 8c. The measured response in these plots is compared with numerical solutions obtained utilizing a software developed for this purpose based on the analytical equations of rocking, as described before. These results are termed in these plots as analytical results. The time step that was adopted was  $DT=0.0001$  sec; this time step was divided by ten ( $DT1=DT/10$ ) just before and after each time the rocking specimen was making full contact with its supporting base.

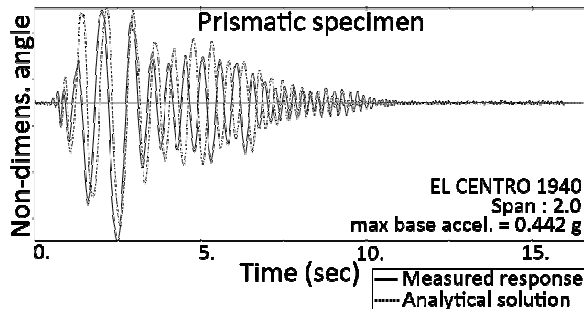


Figure 8a. Measured and analytically predicted rocking response of prismatic specimen Earthquake simulated test Span 2.0

For the tests with intensity Span 2 and Span 3 (figures 8a and 8c) good agreement was achieved between the numerical results based on the analytical equations of rocking and the measured rocking response. However, for the test with simulated earthquake intensity indicator Span 2.5 (figure 8b), the numerical rocking response exhibits large amplification at a time (approximately 6sec.) when the measured response has subsided.

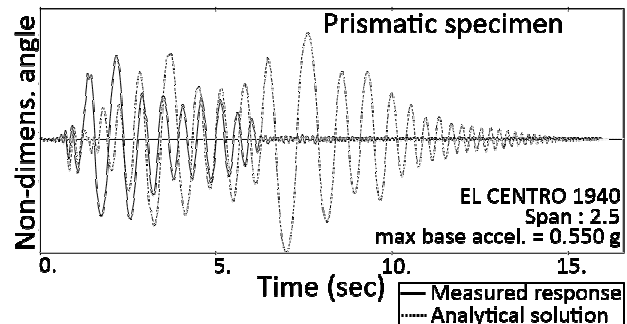


Figure 8b. Measured and analytically predicted rocking response of prismatic specimen Earthquake simulated test Span 2.5

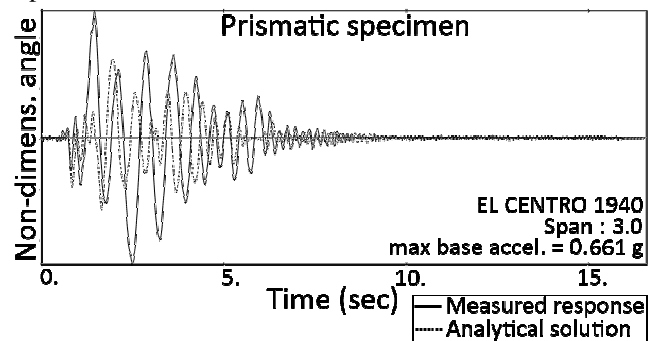


Figure 8c. Measured and analytically predicted rocking response of prismatic specimen Earthquake simulated test Span 3.0

#### 4 NUMERICAL SIMULATION BASED ON A COMMERCIAL SOFTWARE

Initially, the free vibration response of the prismatic specimen, presented in section 2.1., was numerically simulated with the F.E. Abaqus software. At this initial numerical simulation, the influence of the input parameter of the critical damping fraction (CDF) was investigated. This was done by simulating the rocking response of the prismatic specimens with three different discretizations denoted as coarse mesh (1224 DOF) medium mesh (5478 DOF) and fine mesh (20332 DOF). For each one of these three discretizations, the free vibration rocking response of the prismatic specimen was examined, performing for each one of these numerical models (coarse, medium, fine mesh) simulations of the rocking response varying the time step of the non-linear integration scheme. This was done setting the time step equal to one of the following three specific values; that is 100μseconds, 10μseconds and 1μsecond. For each one of these nine basic numerical simulations (with different mesh and different time step) the CDF value was found that results in the best agreement between the Abaqus rocking

predictions of the free vibration rocking behaviour of the prismatic specimen with that obtained by the software based on the analytical equations. This CDF value was found by performing a considerable number of solutions with the Abaqus model through a trial and error process. These values of CDF, that result in the best agreement between the numerical Abaqus results and the analytical results of the free vibration rocking response are included in table 2. It was shown in section 2.1. that the analytically predicted free vibration rocking is in good agreement with the corresponding experimental measurements ([6]), defining indirectly in this way the value of the coefficient of restitution ( $e=0.976$  in the case of the prismatic specimen). As can be seen from the variation of the values of CDF in table 2, when a medium or fine mesh is adopted, with a time step equal or less than  $10\mu\text{seconds}$ , the numerical Abaqus results are in agreement with the analytical results, provided that the parameter CDF is set at a constant value equal to 0.40. Based on this preliminary investigation of the free vibration rocking response of the prismatic model, all the subsequent numerical simulations of the dynamic or simulated earthquake rocking response employed a value for the parameter CDF equal to 0.40. This was done employing at the same time the medium discretization mesh (figure 9) and a time step equal to  $10\mu\text{seconds}$ . As can be seen in figure 10, good agreement could be obtained between the analytical results and the F.E. Abaqus simulation numerical results regarding the free vibration rocking response of the prismatic model.

Mesh	DOF	dt = 100 $\mu\text{s}$		dt = 10 $\mu\text{s}$		dt = 1 $\mu\text{s}$	
		CDF	cost (sec)	CDF	cost (sec)	CDF	cost (sec)
Coarse	1224	1.70	25	0.25	200	0.25	2000
Medium	5478	2.20	70	0.40	600	0.40	6000
Fine	20322	2.60	300	0.40	2700	-	-

Table 2. Values of the critical damping fraction for various mesh schemes and time steps (dt).

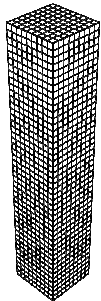


Figure 9. Utilized F.E. mesh

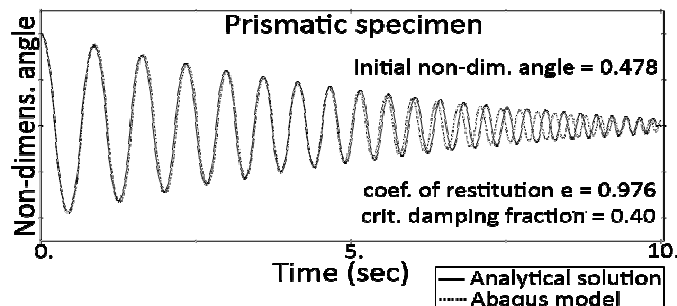


Figure 10. Comparison of numerical results obtained by either the analytical solution or the Abaqus software

#### 4.1. Simulation of Sinusoidal Tests.

A series of numerical simulations with the Abaqus model were performed next using a horizontal base excitation of a sinusoidal type, prescribed by the non-dimensional frequency value  $\Omega_1$  and the non-dimensional amplitude  $A_j$  (see equation 1), as was done in sections 2.2 and 3.1. This sinusoidal base motion is depicted in figure 11, as reproduced by the earthquake simulator of the Laboratory of Strength of Materials and Structures at Aristotle University. The same sinusoidal input motion was also used in the numerical simulations. The obtained results are depicted in figure 12, in the same way as plotted in sections 2 and 3 before, establishing the no rocking-stable rocking boundary as well as the stable rocking-overturning boundary.

These boundary lines are plotted in figure 12 using solid and dashed lines. As was observed in section 3.1. before, the stable rocking-overturning behaviour is depicted with two boundary lines; one corresponds to smaller amplitude values  $A_k$  (lower limit, plotted with a solid line) and a second that corresponds to larger amplitude values  $A_k$  (upper limit, plotted with a dashed line). This again signifies that the results of this type of numerical analysis do not define a single stable rocking - overturning boundary line as was defined by the experimental sequence

The no-rocking-stable rocking boundary is indicated with a solid line that corresponds to non-dimensional amplitude ( $A_k$ ) approximately equal to 1, irrespective of the non-dimensional frequency value ( $\Omega$ ). In the plot of figure 12, the corresponding boundary lines as found from the experimental sequence described in section 2.2 are also plotted. As can be seen very good agreement was obtained between the experimental observations for the stable rocking - overturning boundary (points indicated with the squares) and the corresponding lower limit boundary line predicted by the Abaqus model (plotted with a solid line in figure 12). The very good agreement is also observed between the numerically predicted and the no rocking - stable rocking boundary line established by measurements established by measurements.

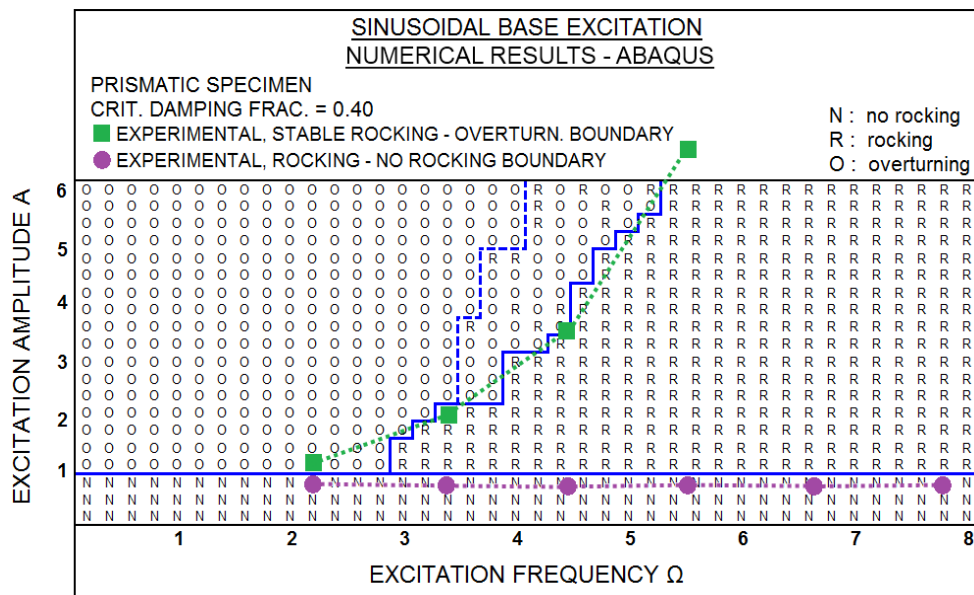


Figure 12. Mapping the stable-unstable rocking response. Numerical predictions with the Abaqus model and experimental measurements

The same comparison is presented in figure 13. This time, apart from the measured (designated as experimental) and the predicted by the Abaqus model boundaries (designated as numerical), the ones obtained by the integration of the analytical equations of rocking, presented in section 3.1. (designated as analytical) are also included. As can be seen, the numerical predictions (lower limit) obtained by the Abaqus model are in better agreement to the observed stable rocking-overturning boundary than the corresponding boundary established by the integration of the analytical equations of rocking

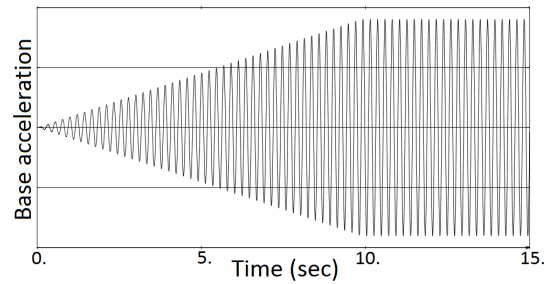


Figure 11. Sinusoidal horizontal base motion used in both the experimental sequence and in the numerical solutions

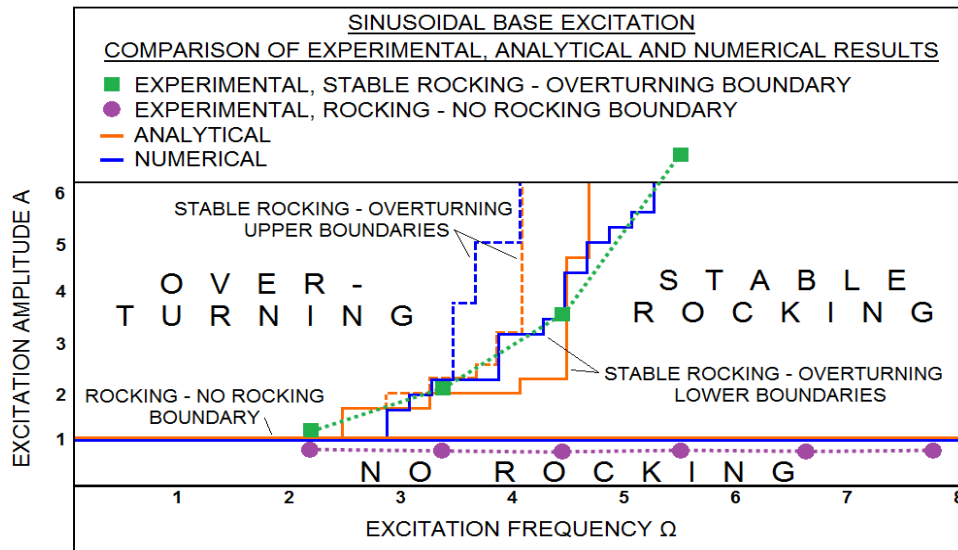


Figure 13. Mapping the stable-unstable rocking response. Numerical predictions with the Abaqus model, the analytical solution and the experimental measurements

## 4.2 Simulated Earthquake tests

A number of numerical simulations were obtained with the Abaqus model and were compared with the rocking response results obtained during the sequence of simulated earthquake tests presented in section 3.2. The intensity of the horizontal base motion is described, as before, by the indicator Span (figures 14).

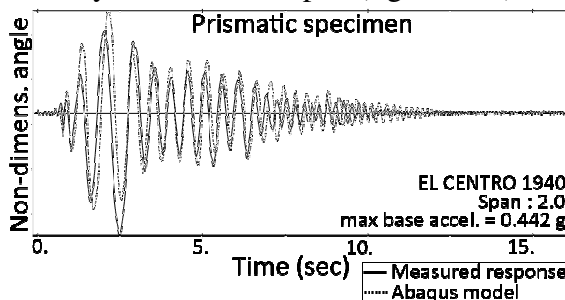


Figure 14a. Measured and numerically predicted rocking response of prismatic specimen Earthquake simulated test Span 2.0

Higher intensity of the simulated earthquake motion corresponds to a larger value for the indicator Span. For the tests with intensity Span 2 and Span 3 (figures 14a and 14c) good agreement was achieved between the numerical results based on the Abaqus model and the measured rocking response. However, for the test with intensity Span 2.5 (figure 14b), the numerical rocking response exhibits large amplification at a time (approximately 6sec.) when the measured response has subsided.

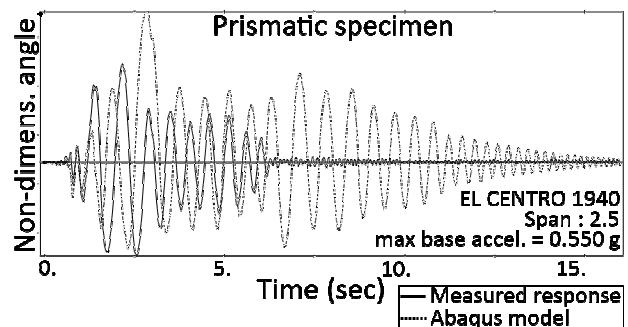


Figure 14b. Measured and numerically predicted rocking response of prismatic specimen Earthquake simulated test Span 2.5

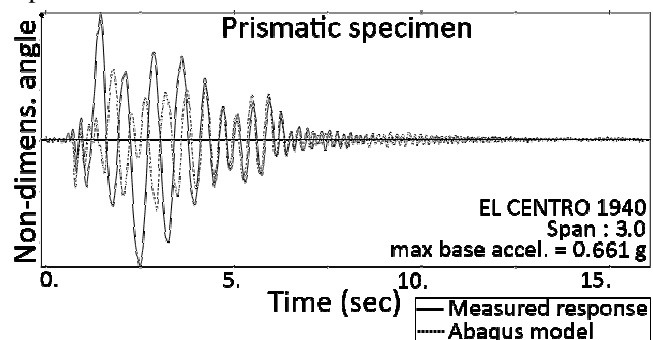


Figure 14c. Measured and numerically predicted rocking response of prismatic specimen Earthquake simulated test Span 3.0

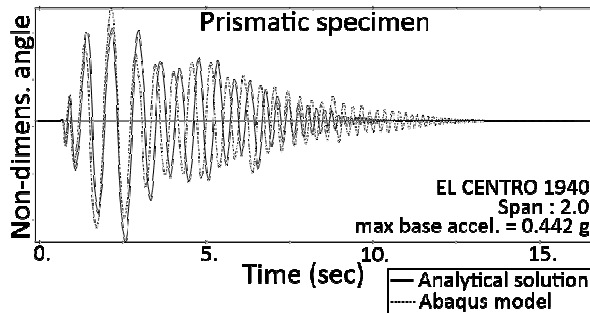


Figure 15a. predicted rocking response (Abaqus model or analytical solution) of prismatic specimen Earthquake simulated test Span 2.0

The same comparison shown in figures 14 is again made in figures 15a to 15c. However, this time instead of the measured rocking response of the prismatic specimen at the shaking table the numerical results obtained either by the Abaqus model or by the analytical equations of motion are shown. The predictions of the rocking response for the prismatic specimen, when subjected to simulated horizontal earthquake excitation, obtained by either the Abaqus model or by the integration of the analytical equations of rocking, exhibit reasonably good agreement.

## 5 CONCLUSIONS

The predicted dynamic rocking performance of a prismatic steel model column was obtained in two different ways. First, through a software that was developed for this purpose, which is based on the integration of the equations of motion that govern the rocking response. Second, utilizing the capabilities of a commercial general purpose software.

The predicted rocking performance, by either the developed software or the commercial software dynamic performance, in terms of stability of the examined prismatic steel model, exhibited similar trends with regard to the influence that the excitation frequency and amplitude of the horizontal sinusoidal base motion exert on its rocking amplitude and its subsequent overturning to the corresponding performance that was observed at the laboratory.

The earthquake rocking response of the examined model prismatic steel column, predicted by either the developed software or the commercial software, in terms of stability and maximum rocking amplitude, exhibited, in general, similar trends to the corresponding performance that was observed at the laboratory.

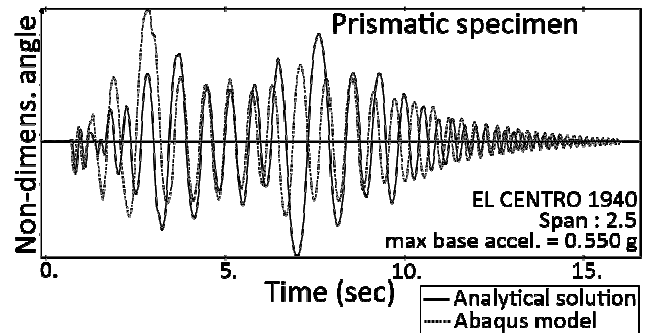


Figure 15b. predicted rocking response (Abaqus model or analytical solution) of prismatic specimen Earthquake simulated test Span 2.5

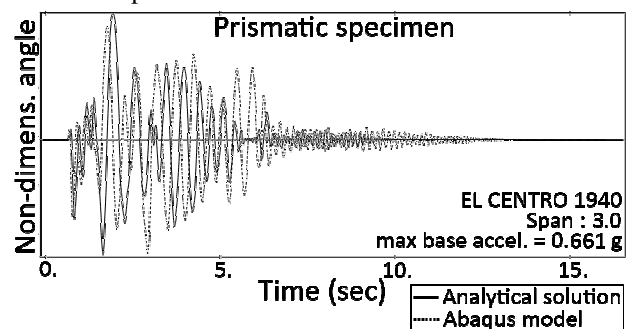


Figure 15c. predicted rocking response (Abaqus model or analytical solution) of prismatic specimen Earthquake simulated test Span 3.0

## REFERENCES

- [1] Aslam , M.M., et.all. 1978. Rocking and Overturning response of rigid bodies to earthquake motions, Report No. LBL-7539, Lawrence Berkeley Lab. Univ. Of California, Berkeley.
- [2] Spanos, P.D. and Koh A.S., 1984. Rocking of rigid blocks due to harmonic shaking. J. of Engin. Mech., ASCE 110 (11), pp. 1627-1642
- [3] Koh, A.S. and Mustafa G. 1990. Free rocking of cylindrical structures, J. of Eng. Mechanics, Vol. 116, N0 1, pp.35-54.
- [4] M. Demosthenous and G.C. Manos : "Dynamic Response of Models of Ancient Monuments Subjected to Horizontal Base motions", IABSE, Struct. Preservation of Archit. Heritage, Italy, 1993, pp. 361-368.
- [5] G.C. Manos and M. Demosthenous : "Comparative Study of the Global Dynamic behaviour of Solid and Sliced Rigid Bodies", 10ECEE, Vienna, Austria, 1994.
- [6] Demosthenous M, 1994. Experimental and numerical study of the dynamic response of solid or sliced rigid bodies, Ph. D. Thesis, Dept. of Civil Engineering, Aristotle University of Thessaloniki.
- [7] Manos, G.C. Reports on Task 1, Task 2 and Task 8, 1998. ISTECH project, Program Environment and Climate, European Commission, Contract No. ENV4-CT95-0106.
- [8] G.C. Manos, M. Demosthenous, V. Kourtides, A. Hatzigeorgiou "The Dynamic and Earthquake Behaviour of Ancient Columns and Colonnades with and without Shape Memory Alloy Devices", STREMAH 2001, Florence, Italy, 2001.
- [9] G.C. Manos et.al "Study of the Dynamic and Earthquake Behaviour of Rigid Bodies with or without the Inclusion of Shape Memory Alloy Devices" , 16SMIRT, Washington D.C. 2001.